‡Equipe Associée au Centre National de la Recherche Scientifique.

[1]T. J. Wieting and J. L. Verble, Phys. Rev. B 5, 1473 (1972).

[2]F. Bassani, D. L. Greenaway, and G. Fisher, in *Physics of Semiconductors: Proceedings of the Seventh International Conference*, edited by M. Hulin (Academic, New York, 1964), p. 51.

[3]J. L. Brebner, J. Phys. Chem. Solids 25, 1427 (1964).

[4]F. Z. Khelladi, Ph. D. thesis, Université Paris VI, 1961 (unpublished).

[5]A. Bourdon and F. Z. Khelladi, Solid State Commun. 9, 1715 (1971).

[6]A. Balzarotti and M. Piacentini, Solid State Commun. 10, 421 (1972).

[7]A. Balzarotti, M. Piacentini, E. Burattini, and P. Picozzi, J. Phys. C: Proc. Phys. Soc., London 4, L273 (1971).

[8]M. Grandolfo, F. Somma, and P. Vecchia, Phys. Rev. B 5, 428 (1972).

[9]A. J. Niilisk and J. J. Kirs, Phys. Status Solidi 31, K91 (1969).

[10]G. A. Akhundov, G. B. Abdullayev, G. D. Guseinov, R. F. Mekhtiev, and M. Kh. Aliyeva, in *Physics of Semiconductors: Proceedings of the Seventh International Conference*, edited by M. Hulin (Academic, New York, 1964), p. 1277.

[11]Y. Nishina, N. Kuroda, and T. Fukoroi, in *Proceedings of the Ninth International Conference on the Physics of Semiconductors, Moscow, U.S.S.R., 1968*, (Nauka, Leningrad, U.S.S.R., 1968), p. 1024.

[12]E. Aulich, J. L. Brebner, and E. Mooser, Phys. Status Solidi 31, 129 (1969).

[13]H. Kamimura, K. Nakao, and Y. Nishina, Phys. Rev. Lett. 22, 1379 (1969).

[14]R. E. Nahory, K. L. Shaklee, R. F. Leheny, and J. C. De Winter, Solid State Commun. 9, 1107 (1971).

[15]E. Lendvay, A. Kuhn, A. Chevy, and T. Ceva, J. Mater. Sci. 6, 305 (1971).

[16]J. C. Phillips, Phys. Rev. Lett. 12, 447 (1964); K. P. Jain, Phys. Rev. 139, A544 (1965).

[17]U. Fano, Phys. Rev. 124, 1866 (1961).

[18]J. C. Irwin, R. M. Hoff, and B. P. Calyman, Solid State Commun. 13, 1531 (1973); J. Reydellet, private communication.

[19]A. Bourdon, Ph. D. thesis, Université de Paris VI, 1971 (unpublished); A. Bourdon, J. Phys. (Paris), Suppl. 35, 217 (1974).

[20]M. Schlueter, Bull. Soc. Suisse Phys. 45, 73 (1972).

[21]J. L. Brebner and E. Mooser, Phys. Lett. 24A, 274 (1967).

[22]J. L. Verble, T. J. Wieting, and P. R. Reed, Solid State Commun. 11, 941 (1972).

Study of Dispersive Raman Modes in Cu_2O by Resonant Raman Scattering

Peter Y. Yu
IBM Thomas J. Watson Research Center, Yorktown Heights, New York 10598

and

Y. R. Shen*
Physics Department, University of California, Berkeley, California 94720, and Inorganic Materials Research Division, Lawrence Berkeley Laboratory, Berkeley, California 94720

(Received 19 February 1974)

We have observed shifts in energy of a number of Raman modes of Cu_2O as a function of incident photon energy. We explain such energy shifts as due to dispersion in the phonons involved and obtain quantitative agreement between theory and experiment. From our data we have also determined the effective mass of the 1*s* yellow exciton in Cu_2O to be $(3.0 \pm 0.2)m_0$.

It is generally accepted[1] that one-phonon Raman modes are characterized by zone-center phonons while multiphonon Raman modes reflect the phonon density of states near critical points. In either case for a given crystal orientation, the Raman frequency shift is independent of the exciting photon energy. In this Letter we report for the first time the observation of some Raman modes in Cu_2O whose frequencies vary with the exciting laser frequency. We have developed a theory to explain our results quantitatively and have shown that it is possible to obtain phonon dispersion relations and the effective mass of the 1*s* exciton band in Cu_2O by resonance Raman scattering (RRS).

Recently Yu *et al.*[2] have shown that RRS of the $2\Gamma_{12}^-$-phonon mode in Cu_2O[3] is dominated by the scattering process shown in Fig. 1(a). For a fixed incident photon energy ω_i, the momentum q of the Γ_{12}^- phonon emitted is determined uniquely

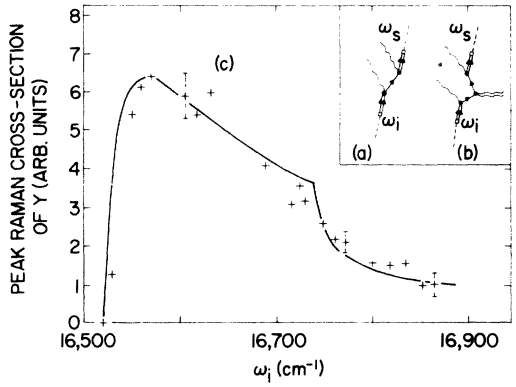

FIG. 1. Schematic representation of the resonant Raman scattering of (a) $2\Gamma_{12}^-$ phonons and (b) $2\Gamma_{12}^-$ + acoustic phonon with the 1s exciton as the intermediate state. Single solid line, 1s yellow exciton; double solid line, β exciton; dashed line, photon; single wavy line, Γ_{12}^- phonon; and double wavy line, acoustic phonon. (c) Peak intensity of the Raman mode Y of Cu_2O as a function of incident photon energy ω_i. The solid curve is a theoretical curve obtained from Eq. (2) [see text].

by the resonance condition

$$\omega_i = \omega_1 + \hbar q^2/2M + \omega_0(q), \quad (1)$$

where ω_1 and ω_0 are respectively the energies of the 1s yellow exciton at $q=0$ and the Γ_{12}^- phonon, and M is the effective mass of the 1s exciton band which is assumed to be spherical. Thus by measuring the energy of the $2\Gamma_{12}^-$ mode as a function of ω_i, one can in principle measure the dispersion curve of the Γ_{12}^- phonon. However, no such shift in the energy of the $2\Gamma_{12}^-$ mode was observed. This is because the Γ_{12}^- mode happens to be almost dispersionless.[4] But there are other phonons in Cu_2O more dispersive than the Γ_{12}^- phonon. This prompted us to measure the position of other Raman peaks of Cu_2O as a function of ω_i. Our measurements were performed at ~2°K in a backscattering configuration using a conventional Raman spectrometer and a cw dye laser[5] on single crystals of Cu_2O grown by oxidation of pure copper and from melt. Results from both kinds of samples are essentially identical. Samples grown from melt have a much stronger luminescence background which tends to obscure the weaker Raman lines. We therefore present here only results obtained from samples grown by oxidation of Cu. Figures 2(a) and 2(b) show two Raman spectra of Cu_2O obtained with two different ω_i. We notice that the peaks labeled Y and Z have clearly shifted in energy with ω_i.

In Fig. 3 we have plotted the peak positions of

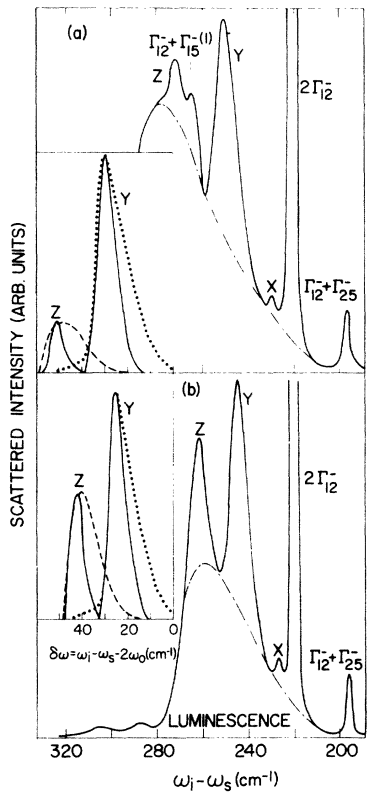

FIG. 2. Raman spectra of Cu_2O for two different incident photon energies: (a) 16 587 cm^{-1} and (b) 16 570 cm^{-1}. The insets show the Raman modes Y and Z after removal of the luminescence background. The dotted and dashed curves are theoretical curves [see text].

all the Raman modes of Cu_2O between 190 and 400 cm^{-1} as a function of ω_i. In this paper we shall consider only the modes X, Y, Z, and $\Gamma_{12}^- + \Gamma_{15}^{-(1)}$ and leave the rest to a more detailed future publication.

We consider the peak Y first because of its comparatively larger cross section. We notice in Fig. 3 that this peak starts by splitting off from the $2\Gamma_{12}^-$ mode (220 cm^{-1}) and shifts to larger values of $\omega_i - \omega_s$ as ω_i increases above the phonon-assisted excitonic absorption edge [$(\omega_1 + \omega_0)/c = 16\,514$ cm^{-1}]. This suggests that this mode is due to scattering of two Γ_{12}^- phonons plus a low-energy dispersive phonon which is presumably a longitudinal acoustic phonon [LA phonons couple more strongly to excitons than TA phonons]. There is also good reason to expect such an acoustic-phonon sideband of the $2\Gamma_{12}^-$ mode. In Ref. 2 it was shown that the damping γ of the 1s yellow exciton with a nonzero momentum q is dominated by the damping γ_{ac} due to emission of an acoustic

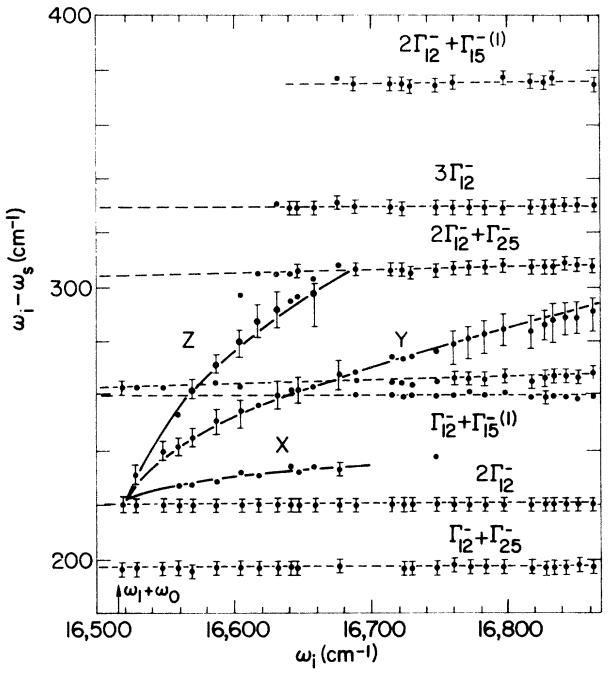

FIG. 3. The position of all the observed Raman modes of Cu_2O between 190 and 400 cm^{-1} as a function of incident photon energy. The broken curves are drawn for clarity. The solid curves are theoretical curves discussed in the text. The vertical bars over the experimental points indicate the half-widths of the corresponding Raman peaks. The position of the absorption edge ($\omega_i + \omega_0$) is indicated by an arrow.

phonon. From the "cascade" theory of Martin and Varma,[6] we expect the ratio of the intensity of this sideband to the intensity of the $2\Gamma_{12}^-$ mode to be $\gamma_{ac}/\gamma \lesssim 1$.

The above interpretation is supported by the following quantitative analysis. Applying perturbation theory to the scattering process shown in Fig. 1(b), we can show that the Raman cross section of the $2\Gamma_{12}^- + \mathrm{LA}(\omega_a(k))$ mode is given by[7]

$$R_Y(\omega_i, \omega_i - \omega_s = 2\omega_0 + \omega_a(k)) \propto \begin{cases} \alpha(\omega_i)\gamma_{ac}(q, k)\gamma^{-2}(q) & 0 \le k \le 2(q - Mv/\hbar), \\ 0 & \text{otherwise}, \end{cases} \tag{2}$$

where $\gamma_{ac}(q, k) \sim k^2[1 + O(k^2)]/q$ is the damping of the $1s$ exciton with momentum q due to emission of LA phonons after summing over all LA phonons with momentum k, $\omega_a(k) = vk$ is the LA phonon frequency, v is the LA phonon velocity, and α is the absorption constant. In order to compare Eq. (1) with the observed Raman spectra we neglect the $O(k^2)$ term in $\gamma_{ac}(q, k)$ and convolute R_y [$\propto \omega_a^2(k)$] with the slit function (which is a Gaussian with a width $\Delta = 3$ cm^{-1}) of the spectrometer. The Raman spectrum is then given by

$$I_Y(\omega_i, \delta\omega = \omega_i - \omega_s - 2\omega_0) \propto \int_0^{2v(q - Mv/\hbar)} d\omega' (\omega')^2 \exp\{-[(\omega' - \delta\omega)/\Delta]^2\}. \tag{3}$$

The dotted curves in the insets of Fig. 2 are calculated from Eq. (3) using $v = 4.15 \times 10^5$ cm/sec for the LA phonons in Cu_2O[8] and M as an adjustable parameter ($M = 2.9m_0$ and $3.2m_0$ for $\omega_i/c = 16\,570$ and $16\,587$ cm^{-1}, respectively). The momemtum q is determined by ω_i from Eq. (1). For all ω_i studied the calculated spectra fit quite well the experimental spectra with $M = (3.0 \pm 0.2)m_0$ except for small values of $\delta\omega$. This discrepancy tends to be bigger for larger ω_i and suggests that the $O(k^2)$ term is significant especially for large k. Using $M = 3.0m_0$ we have computed from Eq. (3) the peak position of the calculated Raman spectrum as a function of ω_i. The theoretical curve, shown as a solid line in Fig. 3, reproduces the experimental peak positions quite well. It is interesting to note that the above value of M is a factor of 2 larger than the effective mass of the higher excited states ($n \ge 2$) of the yellow exciton series deduced from magneto-optical absorption.[9]

As a further check on our theory we have plotted in Fig. 1(c) the peak Raman intensity of Y as a function of ω_i. The solid curve is a plot of Eq. (2) with $k = 2(q - Mv/\hbar)$ and α and $\gamma(q)$ given by their expressions in Ref. 2. In particular we have

$$\gamma \sim \begin{cases} A + (\omega_i - \omega_1 - \omega_0), & \omega_1 + \omega_0 \le \omega_i \le \omega_1 + 3\omega_0; \\ A + (\omega_i - \omega_1 - \omega_0) + B(\omega_i - \omega_1 - 3\omega_0)^{1/2}, & \omega_i \ge \omega_1 + 3\omega_0. \end{cases} \tag{4}$$

For the solid curve in Fig. 1(c) we have used $A = 45$ cm^{-1} and $B \simeq 20$ cm$^{-1/2}$. They agree well with the values of $A \simeq 39$ cm^{-1} and $B \simeq 30$ cm$^{-1/2}$ used to fit the experimental $2\Gamma_{12}^-$ data in Ref. 2.

The change in the peak Z with ω_i is similar to that for peak Y except for its weaker intensity. It is natural to interpret it as a $2\Gamma_{12}^- + 2\mathrm{LA}$ mode. The Raman cross section in this case can be shown to

be

$$R_Z(\omega_i, \omega_i - \omega_s = 2\omega_0 + \omega_a(k_1) + \omega_a(k_2)) \propto \alpha(\omega_i)\gamma_{ac}(q, k_1)\gamma_{ac}(q, k_2)\gamma^{-3}(q) \quad (5)$$

for $0 \leq k_1 \leq 2(q - Mv/\hbar)$ and $0 \leq k_2 \leq 2(q^2 - 2Mvk_1/\hbar)^{1/2} - 2Mv/\hbar$, and zero otherwise. The Raman spectrum is given by

$$I_Z(\delta\omega = \omega_i - \omega_s - 2\omega_0) \propto \int_{\omega_{min}}^{\omega_{max}} d\omega' (\omega')^2(\delta\omega - \omega')^2, \quad (6)$$

with ω_{max} the minimum of $\delta\omega$ and $2v(q - Mv/\hbar)$ and ω_{min} the maximum of 0 and $\delta\omega - 2Mv^2/\hbar - 2v(q^2 - 2M\delta\omega/\hbar)^{1/2}$. The peak position in the Raman spectrum can be calculated numerically from Eq. (6) as a function of ω_i. This is shown as the solid curve in Fig. 3 using $M = 3.0m_0$ obtained from Y and *no adjustable parameter*. The excellent agreement with experiment lends further support to our theory. The corresponding calculated Raman spectra (with peak height normalized to experiment) for $\omega_i/c = 16\,570$ and $16\,587$ cm^{-1} are shown as the dashed curves in the insets of Fig. 2. Again reasonable agreement with experiment is found.

The very weak intensity of the peak X and its otherwise similarity in behavior to Y suggests that it is a $2\Gamma_{12}^- + \text{TA}$ mode. Using the same calculations as we did for the peak Y, but with a TA phonon velocity $= 0.3v$ replacing v, we can predict well the peak position of the X mode as a function of ω_i, as shown by the solid curve in Fig. 3. The TA phonon velocity obtained from the elastic constants[8] is $0.32v$. Unfortunately its weak intensity prevents further quantitative investigation.

Figure 3 also shows that the $\Gamma_{12}^- + \Gamma_{15}^{-(1)}$ mode has a linear splitting with ω_i. According to the phonon dispersion curves of Cu_2O calculated by Carabatos and Prevot,[4] the frequency of the TO component of the $\Gamma_{15}^{-(1)}$ phonon *decreases* linearly while that of the LO component *increases* linearly with q^2. As the dispersion of the Γ_{12}^- phonon is negligible, it is obvious from Eq. (1) that the splitting of the $\Gamma_{12}^- + \Gamma_{15}^{-(1)}$ Raman mode should be proportional to $\omega_i - \omega_1 - \omega_0$ as observed. At $\omega_i/c = 16\,864$ cm^{-1} ($q \sim \frac{1}{4}$ of the Brillouin zone using $M = 3.0m_0$) this TO-LO splitting was found experimentally to be 8 cm^{-1} (as compared to 4 cm^{-1} at $q \approx 0$) while the theoretically predicted splitting is 9 cm^{-1}.

In conclusion we have demonstrated that using RRS it is possible to observe the dispersion of the acoustic and $\Gamma_{15}^{-(1)}$ optical phonons of Cu_2O from zone center out to $\sim \frac{1}{4}$ of the Brillouin zone. We have also determined the effective mass of the $1s$ yellow exciton band to be $(3.0 \pm 0.2)m_0$.

We wish to acknowledge helpful discussions with Dr. F. Stern and Dr. E. Burstein and expert technical assistance from J. Bradley. We are grateful to Professor Y. Petroff for the Cu_2O samples and to Dr. J. E. Smith, Jr., for the Raman spectrometer used in this experiment.

*Research supported by the U. S. Atomic Energy Commission.

[1]See, for example, R. Loudon, Advan. Phys. 13, 423 (1964).

[2]P. Y. Yu, Y. R. Shen. Y. Petroff, and L. Falicov, Phys. Rev. Lett. 30, 283 (1973).

[3]For a review on properties of Cu_2O see S. Nikitine, in *Optical Properties of Solids*, edited by S. Nudelman and S. S. Mitra (Plenum, New York, 1969).

[4]C. Carabatos and B. Prevot, Phys. Status Solidi 44, 701 (1971).

[5]Spectra Physics Model No. 370.

[6]R. M. Martin and C. M. Varma, Phys. Rev. Lett. 26, 1241 (1971).

[7]In our derivation we have assumed the exciton–LA-phonon interaction to be $\propto \sqrt{k}[1 + O(k^2)]$ and the acoustic phonon occupation number $[\exp(\hbar\omega/kT) - 1]^{-1}$ to be $\ll 1$ (since $T \sim 2$°K in our experiment). We have also used Eq. (6) in Ref. 2 whenever the intermediate states are at resonance, thus treating the emission of the acoustic phonons as real transitions which conserve both energy and momentum.

[8]J. Hallberg and R. Hanson, Phys. Status Solidi 42, 305 (1970). The phonon velocities have been averaged over the principal symmetry directions.

[9]A. G. Zhilich, J. Halpern, and B. P. Zakharchenya, Phys. Rev. 188, 1294 (1969). The significance of this difference between the effective masses of the $n = 1$ and $n > 1$ states of the yellow exciton will be discussed in a later publication.